Journal of Physics: Conference Series **393** (2012) 012024 doi:10.1088/1742-6596/393/1/012024

Plasmon nanooptics with individual single wall carbon nanotubes

I. V. Bondarev

Department of Physics, North Carolina Central University, 1801 Fayetteville Str., Durham, NC 27707, USA

E-mail: ibondarev@nccu.edu

M. F. Gelin and W. Domcke

Department of Theoretical Chemistry, Technical University of Munich, Lichtenbergstrasse 4, D-85747 Garching, Germany

Abstract. We discuss how low-energy collective interband plasmon excitations can be used to tune the optical properties of individual single wall carbon nanotubes. Two specific examples are considered. We show that interband plasmons can efficiently mediate enhanced electromagnetic absorption by pristine semiconducting carbon nanotubes and bipartite entanglement in hybrid metallic carbon nanotube systems. We develop a theory for (non-linear) optical monitoring and control of the above phenomena. Our findings pave the way for the development of a new generation of tunable optoelectronic device applications with individual carbon nanotubes.

1. Introduction

Carbon nanotubes (CNs) — graphene sheets rolled-up into cylinders of one to a few nm in diameter and up to one cm in length [1, 2] — have been successfully integrated into miniaturized electronic, electromechanical, and chemical devices [3], scanning probes [4, 5], and into nanocomposite materials [6, 7]. Over the past years, optical nanomaterials research has uncovered intriguing optical attributes of their physical properties, lending themselves to attractive device applications [8, 9, 10]. It is currently realized that pristine semiconducting CNs, which are direct-band semiconductors, can be used both to generate and to detect light [11, 12]. Recent studies of CN based optical nanoscale devices have shown that CNs are able to perform as single-photon sources for quantum computing, communication, or cryptography [13]. Hybrid CN systems containing extrinsic atomic type species (dopants) such as semiconductor quantum dots [14, 15], extrinsic atoms or ions [16, 17], are shown to be promising candidates for the development of the new generation of tunable nanooptoelectronic devices — both application oriented, e.g., photovoltaic devices of improved light-harvesting efficiency [18, 19], and for fundamental research including nanophotonics, nanoplasmonics, cavity quantum electrodynamics, and quantum information [13, 20, 21, 22]. Thus, nanotubes offer a great potential for building a unified optoelectronic technology based on the same material — new technology that, due to the outstanding mechanical and chemical stability of CNs, could be seamlessly integrated into state-of-the-art semiconductor nanotechnology.

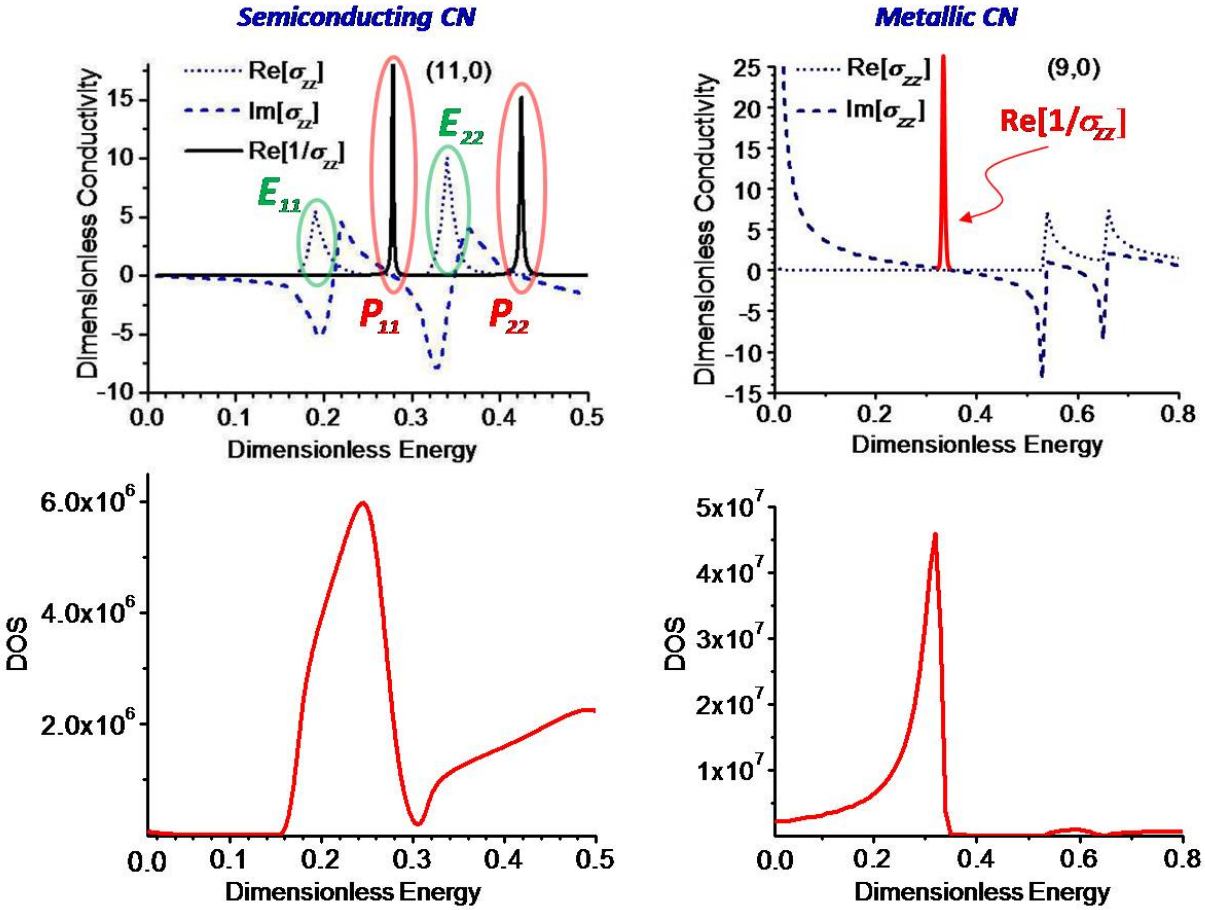

Figure 1. Surface dielectric response functions and local photonic density-of-states (DOS) functions for semiconducting (left panel) and metallic (right panel) CNs. *Top left*: Fragment of the energy dependence of the dimensionless (normalized by $e^2/2\pi\hbar$) axial surface conductivity σ_{zz} of the semiconducting (11,0) nanotube along the CN axis. Ovals mark exciton (E_{11}, E_{22}) and interband plasmon (P_{11}, P_{22}) excitations [peaks of $\mathrm{Re}\,\sigma_{zz}$ and $\mathrm{Re}(1/\sigma_{zz})$, respectively]. *Top right*: Same for the metallic (9,0) nanotube (plasmon resonance not to scale). *Bottom*: Local photonic DOS functions for the semiconducting (11,0) nanotube (left) and metallic (9,0) nanotube (right), when the TLS is placed on the nanotube symmetry axis. Dimensionless energy is defined as $[Energy]/2\gamma_0$, where $\gamma_0 = 2.7$ eV is the C-C overlap integral.

However, the true potential of CN based optoelectronic devices lies in the ability to tune their properties in a controllable way. Here, we discuss how low-energy collective interband plasmon excitations can be used to tune the optical properties of individual single wall CNs. We demonstrate that interband plasmons can efficiently mediate enhanced electromagnetic absorption by pristine semiconducting CNs and bipartite entanglement in hybrid metallic CN systems. We develop a theory for optical monitoring and control of the phenomena above.

2. Pristine semiconducting carbon nanotubes

In general, plasmons cannot be excited by light in optical absorption since they are longitudinal excitations, while photons are transverse. Small-diameter (~ 1 nm) semiconducting CNs, because of their quasi-one-dimensionality (1D), predominantly absorb the external

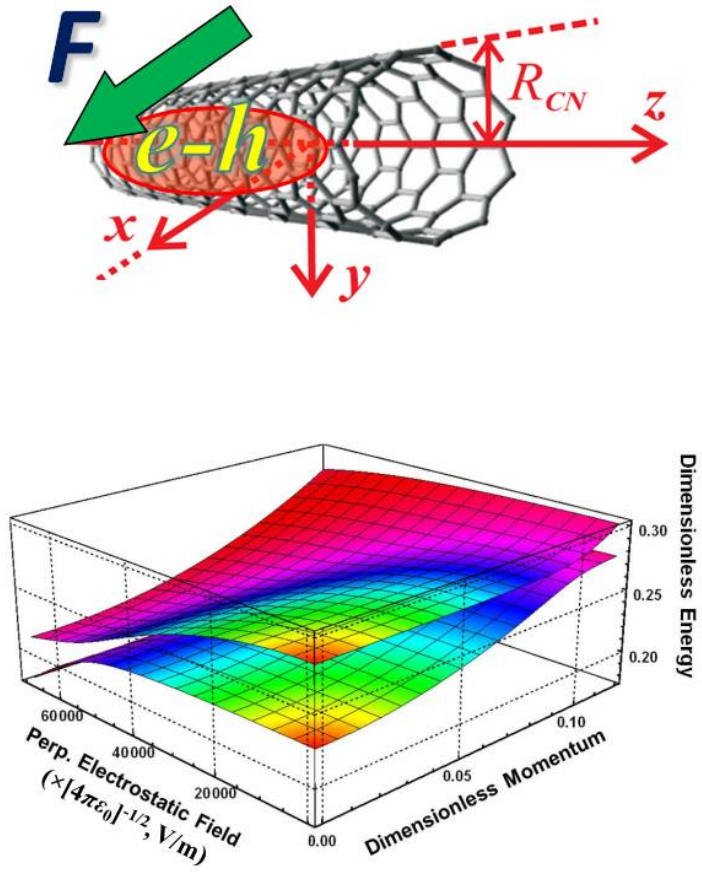

Figure 2. Exciton-plasmon dispersion relation (bottom) as a function of a perpendicular electrostatic field applied (schematic on the top) and longitudinal momentum for the lowest bright exciton [E_{11} in Fig. 1 (top left)] when coupled to the nearest interband plasmon [P_{11} in Fig. 1 (top left)] in the (11,0) nanotube. Dimensionless momentum is defined as $3b\,[Momentum]/2\pi\hbar$, where $b = 1.42$ Å is the C-C interatomic distance. See Fig. 1 caption for the dimensionless energy definition.

electromagnetic (EM) radiation polarized along the CN axis to excite excitons [23]. Figure 1 (top left) shows a typical dynamical dielectric response function for a semiconducting CN [24, 25]. One can see both of the collective excitations, both excitons and interband plasmons, to originate from the same electronic transitions and, therefore, to occur at similar energies (~ 1 eV), as opposed to bulk semiconductors, where they are separated by tens of eVs. These excitations do have different physical nature. Their coexistence in semiconducting CNs is a unique general feature of confined quasi-1D systems where the transverse electronic motion is quantized to form 1D bands and the longitudinal one is continuous.

Optically excited quasi-1D excitons have their transition dipole moments and translational quasi-momenta both directed along the CN axis (z axis of the problem — Fig. 2 (top); cylindrical coordinates are used). Therefore, they can couple to their neighboring longitudinal interband plasmon modes [24, 25]. The exciton-plasmon coupling can be controlled and tuned by means of an electrostatic field applied perpendicular to the CN axis [schematic in Fig. 2 (top)] via the quantum confined Stark effect (QCSE) [24, 26]. Figure 2 (bottom) shows a typical exciton-plasmon dispersion relation in this case [26]. We see the anti-crossing ~ 0.1 eV, both in the energy-momentum plane and in the energy-field plane, revealing the QCSE as an efficient tool to control the exciton-plasmon coupling strength in individual CNs.

The formation of coupled exciton-plasmon excitations can be viewed as an additional non-radiative channel (in addition to phonons [27] and defects [28]) for the exciton relaxation in CNs, where optically excited excitons decay into low-energy interband plasmons. In so doing, excitons generate the quanta of plasma oscillations on the CN surface, on the one hand, and this shortens their lifetime, on the other. Thus, by varying the exciton-plasmon coupling strength

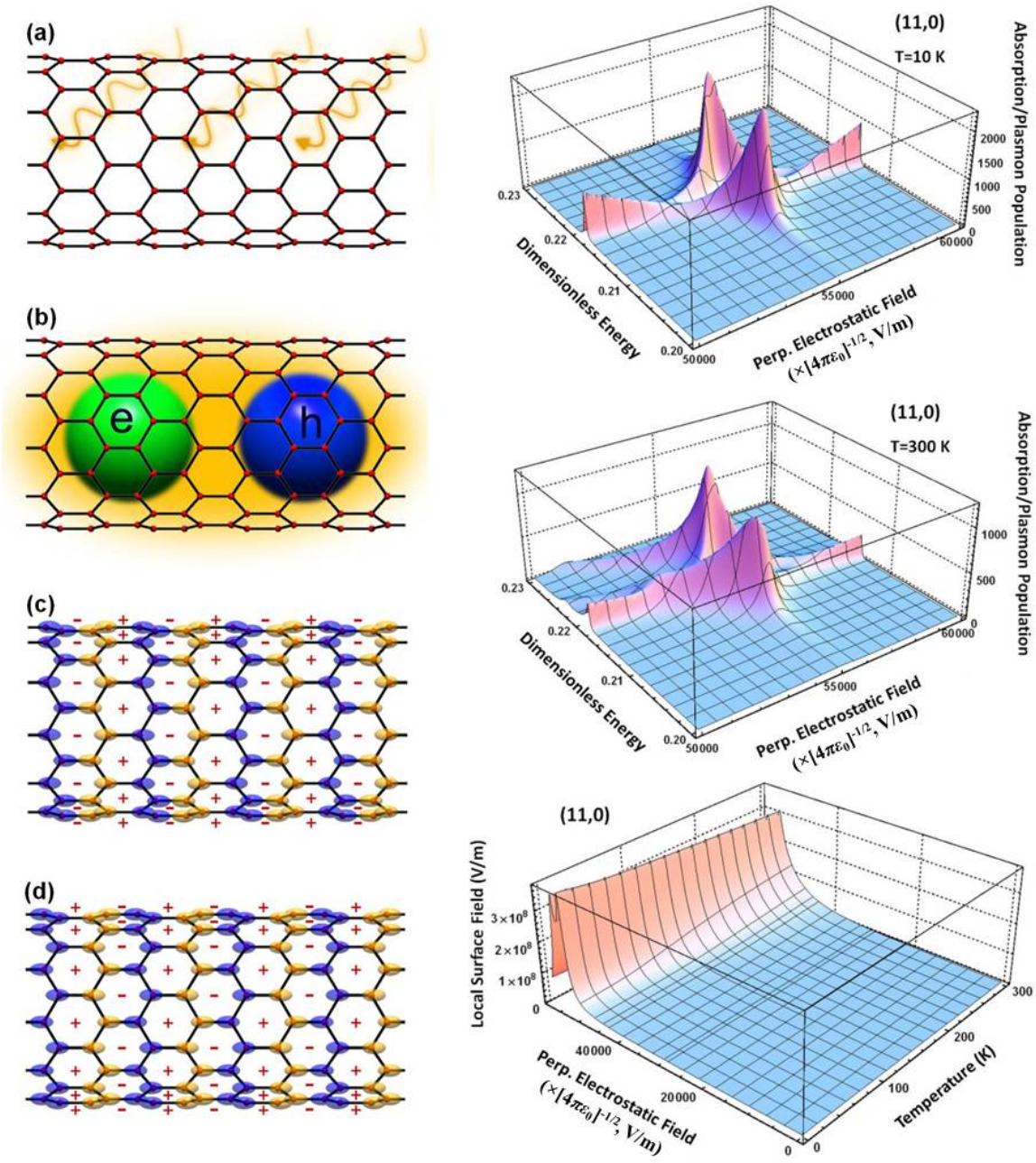

Figure 3. Non-radiative decay of optically excited excitons into plasmons. Calculations for the 1st bright exciton in the (11,0) CN. *Top to bottom left*: Schematic of the plasmon generation by the exciton. *(a),(b)* Exciton excitation by external EM radiation. *(c),(d)* Charge plasma oscillations (shown by + and – signs) produced by the non-radiative exciton decay are periodic opposite-phase displacements of electron shells relative to ion cores in the neighboring elementary cells (blue and yellow) of the CN. *Top to bottom right*: Plasmon population (also representing light absorption by excitons) and local surface field amplitude as functions of temperature and perpendicular electrostatic field applied. See Fig. 1 caption for the dimensionless energy.

using the QCSE, one controls both the radiative emission from an individual CN and surface electric field fluctuations associated with plasmons generated by excitons on the CN surface. This latter phenomenon is similar to the SPASER effect (Surface Plasmon Amplification by Stimulated Emission of Radiation) reported earlier for hybrid metal-semiconductor-dielectric nanomaterials [29]. In our case, the effect takes place in *individual* semiconducting CNs.

Plasma oscillations generated by the non-radiative exciton decay into the nearest interband plasmon mode are *standing* charge density waves due to the periodic opposite-phase displacements of the electron shells with respect to the ion cores in the neighboring elementary cells on the CN surface [Fig. 3 (left)]. Such periodic displacements induce local coherent oscillating electric fields of zero mean, but non-zero mean-square magnitude, concentrated locally across the diameter throughout the length of the nanotube. The mean-square longitudinal local field magnitude can be calculated as the expectation value $E_z^2(\mathbf{n}) = \langle [-\boldsymbol{\nabla}_{\mathbf{n}}\, \hat{\varphi}(\mathbf{n})]_z^2 \rangle$ of the quantum electrodynamical (QED) longitudinal-electric-field operator at the lattice site $\mathbf{n} = \{R_{CN}, \varphi_n, z_n\}$, to result in [26]

$$E_z^2(\mathbf{n}) = \frac{\hbar L}{2\pi^2 c^2 R_{CN}} \sum_{\mathbf{k}=k_\varphi,k_z} f_{ex}(\mathbf{k},T) \int_0^\infty d\omega\, \omega^3\, \mathrm{Re} \frac{1}{\sigma_{zz}(\mathbf{k},\omega)} \left[N(\mathbf{k},\omega) + \frac{1}{2} \right]. \qquad (1)$$

Here, $N(\mathbf{k},\omega) = (4\pi c/L) I(\mathbf{k},\omega)$ is the number of plasmons generated by excitons with the momentum $\mathbf{k} = \{k_\varphi, k_z\}$ of the 1st Brillouin zone on the surface of the tubule of length L [circumferential confinement of the system results in k_φ being quantized to represent electron (e) and hole (h) subbands, while k_z remains continuous to characterize the longitudinal motion of the exciton with the effective mass $M_{ex}(k_\varphi) = m_e(k_\varphi) + m_h(k_\varphi)$], $I(\mathbf{k},\omega) = |C(\mathbf{k},\omega, t\to\infty)|^2$ is the exciton emission intensity distribution written in terms of the probability amplitude $C(\mathbf{k},\omega,t)$ to generate plasmons, and $f_{ex}(\mathbf{k},T) = \exp[-\hbar^2 k_z^2/2M_{ex}(k_\varphi)k_B T]/Q_{ex}$ is the exciton momentum distribution function with the partition function $Q_{ex}(T) = \sum_{\mathbf{k}} \exp[-\hbar^2 k_z^2/2M_{ex}(k_\varphi)k_B T]$.

Equation (1) tells us that in order to produce strong local mean-square fields and related stronger optical absorption by excitons, the exciton emission resonance must overlap with the neighboring plasmon resonance. In other words, in terms of Fig. 1 (top left), the resonance of $\mathrm{Re}\,\sigma_{zz}(\omega)$ at $\omega \sim E_{11}$ [yielding the peak of $N(\mathbf{k}, \omega\sim E_{11}) = (4\pi c/L) I(\mathbf{k}, \omega\sim E_{11})$ in Eq. (1)] must overlap with the resonance of $\mathrm{Re}[1/\sigma_{zz}(\omega)]$ at $\omega \sim P_{11}$. We see in Fig. 2 (bottom) that this can be achieved by carefully tuning the exciton excitation energy and the nearest interband plasmon energy by means of the QCSE. Increasing the perpendicular electrostatic field brings E_{11} and P_{11} closer together, pushing the coupled exciton-plasmon system into the strong coupling regime where all of the optically excited excitons decay non-radiatively to generate interband (same-band) plasmons. This yields the peak optical absorption [Fig. 3 (top and middle right)] due to the efficient exciton-plasmon generation associated with the strong local mean-square fields induced by plasmons throughout the CN surface [Fig. 3 (bottom right)]. As the temperature grows, higher momenta excitons start contributing to the process, lowering the field necessary to achieve the strong coupling regime [blue contrast in Fig. 2 (bottom)].

3. Hybrid metallic carbon nanotube systems

In hybrid CN systems consisting of a metallic nanotube and extrinsic atomic type dopants, such as semiconductor quantum dots [14, 15], extrinsic atoms or ions [16, 17], the long-range EM interaction between the CN and the dopants [modeled by electronic two-level systems (TLS)] is theoretically demonstrated to enter the strong coupling regime as the TLS–CN distance decreases [30]. In the strong coupling regime, the two TLSs, that are properly positioned relative to each other and are close enough to the CN surface, can be significantly entangled even if they are a few tens of Angstroms apart [31]. This bipartite entanglement is due to the strong coupling of each individual TLS to the same surface plasmon resonance of the metallic

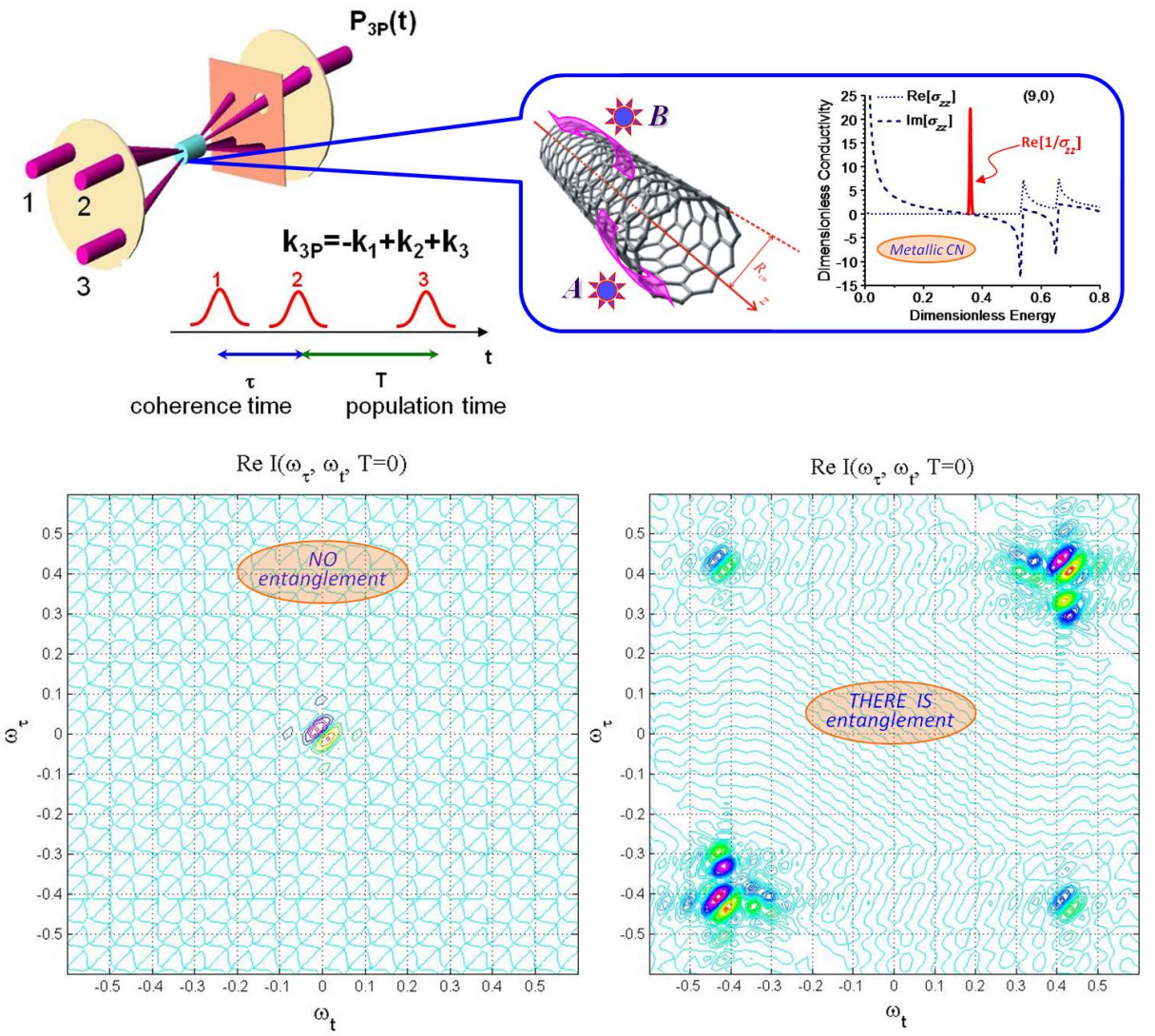

Figure 4. Calculations of the experimental 2D photon-echo signal for hybrid (atomically doped) metallic CN systems. *Top*: Schematic of the optical 2D photon-echo spectroscopy experiment for the detection of the bipartite entanglement between the two spatially separated dipole emitters A and B, which may be a pair of atoms, ions, or quantum dots, coupled to the same surface plasmon resonance mode of a metallic CN (sketch shown in the inset). *Bottom*: 2D optical photon-echo signals calculated in the cases where the bipartite entanglement is absent from (left graph), or present in (right graph) the system. The presence of the cross-peaks on the right panel indicates that the distant dipole emitters are coupled to the same CN surface plasmon resonance and "talk to each other" via the virtual plasmon exchange, being entangled.

CN [see an example in Fig. 1 (top right)]. The coupling is mathematically represented by the strong, sharply peaked, isolated resonance of the local density of photonic states (DOS) typical for metallic, and not for semiconducting, nanotubes (cf. left and right panels in Fig. 1).

Entanglement is a measure of strong quantum correlations (coherences) between quantum objects, which make the wave function of the correlated pair unseparable. To detect the entanglement by optical means, a spectroscopic technique is needed that would allow one to

directly monitor coherences. 2D optical photon-echo spectroscopy has such a potential [32, 33]. To probe our system by means of the 2D optical spectroscopy, we have to consider its interaction with three laser pulses all polarized along the CN axis. It is this laser polarization that is needed to excite the two-level atomic dipole transition in order to couple it to the (same-energy) longitudinally polarized surface EM mode (the plasmon) of the CN. The three laser pulses will excite the TLSs and not the CN, since in metallic nanotubes there are no excitons in the optical spectral range (cf. top left and right panels in Fig. 1). Therefore, for the reasons discussed in Sec. 2 above, no optical laser excitation is possible of metallic CNs by the pulses in question.

Once one of the TLSs is laser-excited, it starts exchanging virtual surface plasmon excitations with its companion a distance away. This will make the spatially separated TLSs entangled (bipartite entanglement) through the coupling of each individual companion to a common coherent interaction energy exchange channel (the CN interband plasmon mode). To make this channel really coherent is not an easy, but doable, task. Indeed, if the TLS transition energy does not originally match the CN photonic DOS resonance [Fig. 1 (bottom right)], then it could still be possible to tune them up by using the QCSE. This narrows the metallic CN first excited band gap [34], shifting the photonic DOS resonance (the interaction energy exchange channel) to the red. At the same time, this leaves the TLS transition energies virtually unaffected (at least to the first order in the perpendicular electrostatic field applied), as they are selected to be excited by the laser field polarized along the CN axis and obey the selection rules that are different from those the perpendicular electrostatic field interaction follows. Thus, if the experiment is properly set up, the 2D photon-echo signal allows one to control and monitor the net response and the degree of the entanglement of the TLS dopants in the hybrid CN system.

In 2D photon-echo spectroscopy [32, 33], one is interested in the third-order non-linear polarization due to three external laser pulses, $P_{3P}(\tau, T, t)$, which obeys the phase-matching condition $\mathbf{k}_{3P} = -\mathbf{k}_1 + \mathbf{k}_2 + \mathbf{k}_3$ [see the schematic in Fig. 4 (top)]. The response signal of the system is then given by the double Fourier transform of the third order polarization

$$I(\omega_\tau, \omega_t, T) = i \int_{-\infty}^{\infty} d\tau dt \, \exp\left(-i\tau\omega_\tau + it\omega_t\right) P_{3P}(\tau, T, t). \tag{2}$$

Figure 4 (bottom) shows the 2D spectra for the (9,0) metallic nanotube with the pair of TLSs coupled to its low-energy plasmon resonance (sketch on the top of Fig. 4). The data are obtained using Eq. (2) and the methods of P_{3P} calculations developed in Ref. [35]. The left graph and the right graph show the spectra for the weak coupling and strong coupling regimes, respectively, with identical TLS–CN coupling constants for both TLSs and no relaxation. (The theory and more details on these calculations will be published elsewhere [36].) The presence of the cross-peaks along with the absence of the pronounced central peak in the 2D spectra are the signatures of the quantum entanglement in the hybrid CN system. The time evolution of the cross-peak intensities allows one to further monitor the entanglement dynamics in the system in the real time scale, thus demonstrating the superior diagnostic power of 2D photon-echo spectroscopy as applied to the phenomena discussed.

4. Conclusion

We consider two examples of how low-energy collective interband plasmon excitations in individual CNs can be used to tune their optical properties. For pristine semiconducting nanotubes, we show that the nonradiative exciton-to-plasmon energy transfer, whereby the external EM radiation absorbed to excite excitons transfers into the energy of surface plasmons, can efficiently mediate and greatly enhance the EM absorption. This enhancement is caused by the buildup of the macroscopic population numbers of coherent localized surface plasmons producing high-intensity local oscillating fields throughout the CN surface. The entire process can be controlled by means of the QCSE. Strong local coherent fields produced in this way can

be used in various new technological applications of individual CNs, such as near-field sensing, optical switching, electromagnetic energy conversion, and materials nanoscale modification.

For hybrid metallic CN systems, we show that 2D photon-echo spectroscopy is a very sensitive tool for detecting the quantum entanglement of a pair of spatially separated, properly positioned dopant TLSs due to their coupling to the same surface plasmon resonance of a metallic CN. This bipartite entanglement can be identified through the presence of cross-peaks in the 2D photon-echo spectra.

Acknowledgments

I.V.B. is supported by the US DOE (DE-SC0007117) and US ARO (W911NF-11-1-0189). M.F.G. and W.D. acknowledge support from the DFG-Cluster of Excellence "Munich-Centre for Advanced Photonics (MAP)" (www.munich-photonics.de). I.V.B is partially supported by MAP.

References

[1] Dresselhaus M, Dresselhaus G and Avouris Ph (eds) 2001 *Carbon Nanotubes: Synthesis, Structure, Properties, and Applications* (Berlin: Springer-Verlag)
[2] Zheng L X, *et al* 2004 *Nature Materials* **3**, 673
[3] Baughman R H, Zakhidov A A and de Heer W A 2002 *Science* **297**, 787
[4] Popescu A, Woods L M and Bondarev I V 2008 *Nanotechnology* **19** 435702
[5] Popescu A and Woods L M 2009 Appl. Phys. Lett. **95** 203507
[6] Han J-H, *et al* 2010 Nature Materials **9** 833
[7] Dang X, Yi H, Ham M-H, Qi J, Yun D S, Ladewski R, Strano M S, Hammond P T and Belcher A M 2011 *Nature Nanotechnology* **6** 377
[8] Hertel T 2010 *Nature Photonics* **4** 77
[9] Avouris Ph, Freitag M and Perebeinos V 2008 *Nature Photonics* **2** 341
[10] Avouris Ph and Chen J 2006 *Materials Today* **9** 46 (2006)
[11] Mueller T, Kinoshita M, Steiner M, Perebeinos V, Bol A A, Farmer D B Avouris Ph 2010 *Nature Nanotechnology* **5** 27
[12] Xia F, Steiner M, Lin Y-M and Avouris Ph 2008 *Nature Nanotechnology* **6** 609
[13] Högele A, Galland Ch, Winger M and Imamoğlu A 2008, Phys. Rev. Lett. **100** 217401
[14] Olek M, Busgen T, Hilgendorff M and Giersig M 2006 *J. Phys. Chem.* B **110** 12901
[15] Haremza J M, Hahn M A and Krauss T D 2002 *Nano Lett.* **2** 1253
[16] Jeong G-H, Farajian A A, Hatakeyama R, Hirata T, Yaguchi T, Tohji K, Mizuseki H and Kawazoe Y 2003 *Phys. Rev.* B **68** 075410; *Thin Solid Films* **435** 307
[17] Khazaei M, Farajian A A, Jeong G-H, Mizuseki H, Hirata T, Hatakeyama R and Kawazoe Y 2004 *J. Phys. Chem.* B **108** 15529
[18] Robel I, Bunker B A and Kamat P V 2005 *Advanced Materials* **17** 2458
[19] Vietmeyer F, Seger B and Kamat P V 2007 *Advanced Materials* **19** 2935
[20] Steiner M, Freitag M, Perebeinos V, Naumov A, Small J, Bol A A and Avouris Ph 2009 *Nano Lett.* **9** 3477
[21] Bondarev I V 2010 *J. Comp. Theor. Nanosci.* **7** 1673
[22] Popescu A, Woods L M and Bondarev I V 2011 *Phys. Rev.* B **83** 081406(R)
[23] Ando T 2005 *J. Phys. Soc. Jpn.* **74** 777
[24] Bondarev I V, Woods L M and Tatur K 2009 *Phys. Rev.* B **80** 085407
[25] Bondarev I V, Tatur K and Woods L M 2009 *Opt. Commun.* **282** 661
[26] Bondarev I V 2012 *Phys. Rev.* B **85** 035448
[27] Perebeinos V, Tersoff J and Avouris Ph. 2005 *Phys. Rev. Lett.* **94** 027402
[28] Hagen A, Steiner M, Raschke M B, Lienau C, Hertel T, Qian H, Meixner A J and Hartschuh A 2005 *Phys. Rev. Lett.* **95** 197401
[29] Bergman D J and Stockman M I 2003 *Phys. Rev. Lett.* **90** 027402
[30] Bondarev I V and Vlahovic B 2006 *Phys. Rev.* B **74** 073401
[31] Bondarev I V and Vlahovic B 2007 *Phys. Rev.* B **75** 033402
[32] Cho M 2009 *Two-Dimensional Optical Spectroscopy* (Boca Raton: Taylor & Francis)
[33] Abramavicius D, Palmieri B, Voronine D V, Sanda F and Mukamel S 2009 *Chem. Rev.* **109** 2350
[34] O'Keeffe J, Wei C and Cho K 2002 *Appl. Phys. Lett.* **80** 676
[35] Gelin M F, Egorova D and Domcke W 2009 *Acc. Chem. Res.* **42** 1290
[36] Gelin M F, Bondarev I V and Meliksetyan A V 2012 *Chemical Physics* (at print)